Algebraic theory of endohedrally confined diatomic molecules: Application to H$_2$@C$_{60}$

Lorenzo Fortunato

Dipartimento di Fisica e Astronomia "G. Galilei", Università di Padova and I.N.F.N.- Sez. di Padova; via Marzolo, 8, I-35131, Padova, Italy

Francisco Pérez-Bernal

Grupo de Investigación en Física Molecular, Atómica y Nuclear (GIFMAN-UHU), Unidad Asociada al CSIC. Departamento de Ciencias Integradas, Universidad de Huelva, 21071 Huelva, Spain

A simple and yet powerful approach for modeling the structure of endohedrally confined diatomic molecules is introduced. The theory, based on a u(4) ⊕ u(3) dynamical algebra, combines u(4), the vibron model dynamical algebra, with a u(3) dynamical algebra that models a spherically symmetric three-dimensional potential. The first algebra encompasses the internal rotovibration degrees of freedom of the molecule, while the second takes into account the confined molecule center-of-mass degrees of freedom. A resulting subalgebra chain is connected to the underlying physics and the model is applied to the prototypical case of H$_2$ caged in a fullerene molecule. The spectrum of the supramolecular complex H$_2$@C$_{60}$ is described with a few parameters, and predictions for not yet detected levels are made. Our fits suggest that the quantum numbers of a few lines should be reassigned to obtain better agreement with data.

I. INTRODUCTION

Supramolecular species in which a guest atom or molecule is inserted in the interior of a host molecule (usually fullerenes) are known as endohedral compounds, and form systems that are bound by the pure confinement rather than by intramolecular forces. The first endohedral compounds obtained consisted of trapped metal atoms [1] followed by endofullerenes with a trapped molecule [2]. These systems display a full gamut of quantum effects, because the confinement of the molecule results in the splitting of the translational degrees of freedom of the incarcerated molecule center of mass and their coupling with rotovibrational ones. A fundamental breakthrough that has allowed the application of different spectroscopic tools to molecular endofullerenes has been the achievement of high reaction yields in their synthesis using the so-called molecular surgery (see, e.g., Refs. [3,4] and references therein). Komatsu and coworkers have presented the synthesis of the endohedral species H$_2$@C$_{60}$, which is the subject of the present work [5]. Another impressive step forward in this area has been Murata's group achievement, using similar experimental techniques, of the synthesis of a closed water endofullerene [6] and the recent encapsulation of hydrogen fluoride inside C$_{60}$ [7].

Significant experimental and theoretical research efforts have been devoted to the elucidation of the spectral properties of H$_2$@C$_{60}$ due to the remarkable quantum effects that link rotovibrational and translational degrees of freedom, coming into play once the diatomic molecule is trapped into the buckyball. In the case of incarcerated H$_2$, the well-known existence of two allotropes of the hydrogen molecule, *para*-H$_2$ and *ortho*-H$_2$, make this compound a valuable tool for explorations in spin chemistry [8]. These fascinating characteristics of the supramolecular complex H$_2$@C$_{60}$ have stimulated remarkable experimental efforts with different techniques [3,9], mainly nuclear magnetic resonance (NMR) [5,8,10], infrared (IR) [11–13], and inelastic neutron scattering (INS) [14–18]. In particular, an INS spectroscopy selection rule of H$_2$@C$_{60}$

has been recently discovered [17,19,20]. The search for an adequate description of the structure and the peculiar properties of this endohedral species has provoked intense theoretical efforts [19–24]. This system represents an almost ideal testing ground for theories because it couples the simplest diatomic molecule with an almost perfect spherical cage (the icosahedral symmetry can be neglected for most practical purposes). The neutral molecule retains its bound character but, at the same time, it is affected by the presence of the fullerene: its motion is confined and quantized due to the interaction with the cage, a situation that can be fully explored by powerful and simple symmetry-guided models.

Measurements of the IR spectrum of H$_2$@C$_{60}$ from low temperatures up to room temperatures have been performed [11–13]. Combining IR spectroscopy data and INS results, the lowest portion of the endohedral compound spectrum has been measured with sufficient detail to allow the experimental underpinning of the differences, shifts, and splitting of the levels with respect to the free H$_2$ counterpart. The spectrum of the confined H$_2$ molecule has been interpreted in terms of a very accurate, though computationally involved, five-dimensional phenomenological model [21–24]. While these five-dimensional calculations are accurate and can be used to conveniently describe the observations and to make guesses about still unobserved excited states, it is not completely obvious what is the origin of the perturbations in the potential energy terms. For example in [22] the authors use Lennard-Jones potentials for each H-C pair in the complex, realizing that the use of an angular momentum quantum number associated with a harmonic motion of the molecule inside the cage is indeed appropriate. This fact supports the convenience of a computationally inexpensive symmetry-based approach like the one we suggest.

We will describe our algebraic approach in Sec. II, discuss the methodology and the fits to a set of experimental lines in Sec. III, and draw conclusions in Sec. IV.

II. ALGEBRAIC APPROACH

Stimulated by the success of the existing approach [11,12], with the aim of obtaining a simple model that encompasses the main physical ingredients for such an enticing system, we propose an algebraic theory for the quantum modes of a diatomic molecule confined in an isotropic three-dimensional cage. Symmetry considerations constitute the guiding principle that inspires the treatment of the energy terms obtained from a Hamiltonian operator that includes molecular rotovibrational and center-of-mass modes, and the coupling of these two subsystems. The rotations and vibrations of the diatomic molecule are described within the vibron model [25–27], which amounts to a u(4) Lie algebra arising from the bilinear products of scalar $s, s^\dagger$ ($\ell = 0$) and vector $p_\mu, p_\mu^\dagger$ ($\ell = 1, \mu = \pm 1, 0$) boson operators [25]. The fullerene cage is modeled as a spherical three-dimensional well and can be dealt with a u(3) Lie algebra, arising from a vector boson operator $q_\mu, q_\mu^\dagger$ ($\ell = 1, \mu = \pm 1, 0$) [28]. Taking this into consideration we invoke an algebraic model based on the direct sum Lie algebra $u_p(4) \oplus u_q(3)$ to describe the intrinsic modes of excitations of the supramolecular complex $H_2@C_{60}$, where we use the subindexes p and q to distinguish the two different sets of degrees of freedom. Our symmetry-inspired scheme should be desirable for at least the following peculiar features: (i) it gives a simple framework that singles out what are the linearly independent energy terms and their connection with physical operators; (ii) it gives a natural explanation for the interaction between translational and rotovibrational degrees of freedom responsible for term energy splittings; (iii) it also gives a natural explanation for the specific radial and angular

dependence ($\{R, \Omega, \Omega_s\}$ in the notation of Refs. [11,12]) of the terms that have been found to contribute to the expansion of the coupling potential function; (iv) it treats on an equal footing *para*- and *ortho*-H_2 states; (v) there is no need to find separate sets of parameters for each vibrational band, a single fit encompasses all vibrational states simultaneously; and (vi) it is computationally inexpensive: the matrix elements of each operator are known in closed form and the diagonalization can be performed exactly and rapidly. In addition, it yields precise predictions for higher lying modes that, although unseen heretofore, might be investigated in the future.

A model that shares a similar algebraic structure, with a dynamical algebra u(7) ⊃ u(3) ⊕ u(4), has been used in the description of hadronic structure in terms of quark building blocks [28,29]. In that model the u(7) algebra arises from two Jacobi coordinate vectors that describe quarks inside a baryon plus a scalar boson and it is used for the spatial part of the description that must be supplemented by a fermionic part containing the flavor, spin, and color degrees of freedom. While the algebraic structure is very similar, clearly the physics behind the model is completely different.

Our model provides a complete mathematical characterization of all possible interactions that comply with the underlying symmetries and therefore naturally gives a hint of the various physical mechanisms that might generate them. We will confine the present discussion to identifying the most important terms and return to the laborious task of a complete classification in a longer paper [30].

Among the many possible subalgebra chains, we consider the following dynamical symmetry:

$$
\begin{array}{cccccccc}
u_p(4) \oplus u_q(3) \supset so_p(4) & \oplus & u_q(3) \supset so_p(3) & \oplus & so_q(3) \supset so_{pq}(3) \supset so_{pq}(2), \\
N_p \quad N_q \quad \omega & & J & & L \quad \Lambda \quad M_\Lambda
\end{array}
\tag{1}
$$

where we have used the so(4) limit of the vibron model [25–28] and where the second line gives the quantum numbers associated with the Casimir operators of each algebra. With the *proviso* that ω is related to the vibrational quantum number v through $v = \frac{1}{2}(N_p - \omega)$, the set $(v J N_q L \Lambda)$ corresponds to the quantum numbers used so far in theoretical investigations. The basis states can therefore be labeled, very similarly to Refs. [9,11,12,14,15,21,22,31], as $|N_p v J; N_q L; \Lambda\rangle$.

The quantum numbers follow the well-known branching rules [27,28]

$$
\begin{aligned}
\omega &= N_p, N_p - 2, \ldots, 1 \text{ or } 0, \\
J &= 0, 1, \ldots, \omega, \\
L &= N_q, N_q - 2, \ldots, 1 \text{ or } 0, \\
\Lambda &= |J - L|, |J - L| + 1, \ldots, J + L. \\
M_\Lambda &= -\Lambda, -\Lambda + 1, \ldots, \Lambda - 1, \Lambda.
\end{aligned}
\tag{2}
$$

The total Hamiltonian can be written as

$$
\hat{H}_{\text{endo}} = \hat{H}_{u_p(4)} + \hat{H}_{u_q(3)} + \hat{H}_{\text{coupl}},
\tag{3}
$$

where the first term represents the vibron model Hamiltonian for rotations and vibrations of a diatomic molecule [26], the second is the quantized motion of the molecular center-of-mass

inside the three-dimensional spherically symmetric confining potential, and the last term includes molecule-cage couplings.

The u(4) vibron model Hamiltonian can be modeled as

$$
\hat{H}_{u_p(4)} = \hat{H}_{so(4)} + \hat{H}_{\text{Dun}},
\tag{4}
$$

where the first term contains the two-body Casimir operators of the so(4) dynamical symmetry and the second includes two higher-order terms in a Dunham-like expansion [26,27] where the first term represents a centrifugal correction and the second a rotation-vibration coupling:

$$
\hat{H}_{so(4)} = E_0 + \beta \hat{C}_2[so_p(4)] + \gamma \hat{C}_2[so_p(3)],
\tag{5}
$$

$$
\hat{H}_{\text{Dun}} = \gamma_2 \hat{C}_2[so_p(3)]^2 + \kappa \hat{C}_2[so_p(4)]\hat{C}_2[so_p(3)].
\tag{6}
$$

The Casimir operators in Eqs. (5) and (6) are diagonal in the chosen basis (1):

$$
\begin{aligned}
\langle \alpha | \hat{C}_2[so_p(4)] | \alpha \rangle &= \omega(\omega + 2), \\
\langle \alpha | \hat{C}_2[so_p(3)] | \alpha \rangle &= J(J + 1), \\
\langle \alpha | \hat{C}_2[so_p(4)]\hat{C}_2[so_p(3)] | \alpha \rangle &= \omega(\omega + 2)J(J + 1),
\end{aligned}
\tag{7}
$$

where $|\alpha\rangle = |N_p v J; N_q L; \Lambda\rangle$.

The energy formula obtained for $\hat{H}_{u_p(4)}$ is

$$E_{u_p(4)} = E_0 + \beta\,\omega(\omega + 2) + \gamma\,J(J + 1)$$
$$+ \gamma_2[J(J + 1)]^2 + \kappa\,[\omega(\omega + 2)J(J + 1)], \quad (8)$$

where $\omega = N_p, N_p - 2, \ldots, 1$ or 0 or, alternatively, $v = 0, 1, \ldots, \frac{1}{2}(N_p - 1)$ or $\frac{1}{2}N_p$ and $J = 0, 1, \ldots, \omega$. The parameters in Eq. (8) are free parameters that can be adjusted to optimize the agreement with experimental data and can be put in direct correspondence with those defined in the approach of Refs. [11,12].

The center-of-mass degrees of freedom Hamiltonian, within the $u_q(3)$ dynamical symmetry, is

$$\hat{H}_{u_q(3)} = a\,\hat{C}_1[u_q(3)] + b\,\hat{C}_2[u_q(3)] + c\,\hat{C}_2[so_q(3)], \quad (9)$$

where the first term is the number of q bosons (and would be the only term if the confining potential were an isotropic three-dimensional harmonic oscillator), the second term is an anharmonic correction, and the third term is the H_2 center-of-mass centrifugal energy.

Again the Casimir operators are diagonal in the chosen basis,

$$\langle\alpha|\hat{C}_1[u_q(3)]|\alpha\rangle = N_q,$$
$$\langle\alpha|\hat{C}_2[u_q(3)]|\alpha\rangle = N_q^2, \quad (10)$$
$$\langle\alpha|\hat{C}_2[so_q(3)]|\alpha\rangle = L(L + 1),$$

where $|\alpha\rangle = |N_p v J; N_q L; \Lambda\rangle$. The free parameters are a, b, and c and the spectrum associated with the center-of-mass degrees of freedom can be written in this approach as

$$E_{u_q(3)} = a\,N_q + b\,N_q^2 + c\,L(L + 1), \quad (11)$$

where N_q is the eigenvalue of the number of quanta operator and L is the orbital angular momentum of the whole confined particle (viz. the center of mass of the H_2 molecule) inside the fullerene cage.

A. Diatomic molecule and spherical cage coupling

The guest diatomic molecule and the cage interact through a number of different physical mechanisms that can be traced back to scalar operators built out of the elements of the different algebras. Even at this level, the model is quite rich, therefore one needs to select the most important operators guided by some physical principle and intuition, rather than looking for global fits that would entail too many parameters. We have found that the relevant terms imply quadrupole-quadrupole couplings.

The algebraic scheme entails two sets of quadrupole operators, namely, $\hat{Q}_p = [p^\dagger \times \tilde{p}]^{(2)}$, the quadrupole operators of $u_p(4)$, and $\hat{Q}_q = [q^\dagger \times \tilde{q}]^{(2)}$, the quadrupole operators of $u_q(3)$. The former describes the intrinsic (non-null if $J \neq 0$) quadrupole of the H_2 molecule, while the latter can be associated with the quadrupole deformation of the probability amplitude of the whole molecule inside the spherical cage. A scalar coupling can be built from these two operators as $[\hat{Q}_p^{(2)} \times \hat{Q}_q^{(2)}]^{(0)}$, which is the basis for the coupling term in the Hamiltonian (3). In addition, following the spirit of a Dunham expansion, further terms can be considered that lead us to selecting the following coupling Hamiltonian:

$$\hat{H}_{coupl} = \vartheta_{pq}\big[\hat{Q}_p^{(2)} \times \hat{Q}_q^{(2)}\big]^{(0)} + \vartheta_{pqw}\big\{\hat{C}_2[so_p(4)]\big[\hat{Q}_p^{(2)} \times \hat{Q}_q^{(2)}\big]^{(0)} + \big[\hat{Q}_p^{(2)} \times \hat{Q}_q^{(2)}\big]^{(0)}\hat{C}_2[so_p(4)]\big\} + v_{pq}\hat{C}_1[u_q(3)]\hat{C}_2[so_p(4)].$$
$$(12)$$

The parameters ϑ_{pq}, ϑ_{pqw}, and v_{pq} can be used to adjust the interaction strengths. The most important finding about the $[\hat{Q}_p^{(2)} \times \hat{Q}_q^{(2)}]^{(0)}$ quadrupole-quadrupole interaction is that it lifts the degeneracy of $\Lambda \neq 0$ multiplets, giving the correct and unusual ordering seen in experiments. For example, the triplet of states with $J = 1$, $N_q = L = 2$ has the ordering $\Lambda = 2, 3, 1$ that cannot be due to a scalar coupling of the rotational and translational angular momentum. In fact, once J (the rotational angular momentum) and L (the translational angular momentum) are set, a term of the form $\vec{J} \cdot \vec{L}$ always gives a splitting of the levels $|J - L| < \Lambda < J + L$ that strictly follows an increasing or decreasing ordering depending on the sign of the strength constant.

Following the appendix of Ref. [32] or Ref. [33], the matrix elements of the scalar coupling of the $\hat{Q}_p$ and $\hat{Q}_q$ quadrupole operators are

$$\big\langle N_p\omega J; N_q L; \Lambda\big|\big[\hat{Q}_p^{(2)} \times \hat{Q}_q^{(2)}\big]^{(0)}\big|N_p\omega'J'; N_q'L'; \Lambda'\big\rangle$$
$$= (-1)^{L+\Lambda+J'}\sqrt{5}\begin{Bmatrix} J & L & \Lambda \\ L' & J' & 2 \end{Bmatrix}\langle N_q L||\hat{Q}_q||N_q'L'\rangle\langle\omega J||\hat{Q}_p||\omega'J'\rangle\delta_{\Lambda,\Lambda'}. \quad (13)$$

Once we separate the molecular and cage degrees of freedom, the reduced matrix elements of the molecular ($\hat{Q}_p$) and center-of-mass ($\hat{Q}_q$) quadrupole degrees of freedom are [27]

$$\langle N_q L||\hat{Q}_q||N_q L\rangle = (2N_q + 3)\sqrt{\frac{L(L + 1)(2L + 1)}{6(2L - 1)(2L + 3)}},$$

$$\langle N_q L + 2||\hat{Q}_q||N_q L\rangle = \sqrt{\frac{(N_q - L)(N_q + L + 3)(L + 1)(L + 2)}{(2L + 3)}},$$

$$\langle\omega 0||\hat{Q}_p||\omega 0\rangle = 0,$$

$$\langle \omega J || \hat{Q}_p || \omega J \rangle = (N_p + 2)\left(1 + \frac{J(J+1)}{\omega(\omega+2)}\right)\sqrt{\frac{J(J+1)(2J+1)}{6(2J-1)(2J+3)}},$$

$$\langle \omega J + 2 || \hat{Q}_p || \omega J \rangle = (N_p + 2)\sqrt{\frac{(\omega-J-1)_2(\omega+J+2)_2(J+1)(J+2)}{4\omega^2(\omega+2)^2(2J+3)}},$$

$$\langle \omega + 2 J - 2 || \hat{Q}_p || \omega J \rangle = \sqrt{\frac{(N_p-\omega)(N_p+\omega+4)(\omega-J+1)_4 J(J-1)}{16(\omega+1)_3(\omega+2)(2J-1)}},$$

$$\langle \omega + 2 J || \hat{Q}_p || \omega J \rangle = \sqrt{\frac{(N_p-\omega)(N_p+\omega+4)(\omega-J+1)_2(\omega+J+2)_2 J(J+1)(2J+1)}{24(\omega+1)_3(\omega+2)(2J-1)(2J+3)}},$$

$$\langle \omega + 2 J + 2 || \hat{Q}_p || \omega J \rangle = \sqrt{\frac{(N_p-\omega)(N_p+\omega+4)(\omega+J+2)_4(J+1)(J+2)}{16(\omega+1)_3(\omega+2)(2J+3)}},$$

where we introduce the Pochhammer symbol $(a)_b = a(a + 1)\cdots(a + b - 1)$.

The matrix elements for the other two operators in the coupling term (12), $\{\hat{C}_2[\text{so}_p(4)][\hat{Q}_p^{(2)} \times \hat{Q}_q^{(2)}]^{(0)} + [\hat{Q}_p^{(2)} \times \hat{Q}_q^{(2)}]^{(0)}\hat{C}_2[\text{so}_p(4)]\}$ and $\hat{C}_1[u_q(3)]\hat{C}_2[\text{so}_p(4)]$ are trivially computed using Eqs. (7), (10), and (13).

Another relevant consideration with regard to the quadrupole-quadrupole coupling is the following: if one defines a total quadrupole operator as the sum of the two effects, $\hat{Q}_T = \hat{Q}_p + \hat{Q}_q$, and takes the ratio of the expectation values of this in the first two excited states, namely, $|A\rangle = |00111\rangle$ and $|B\rangle = |01001\rangle$, the resulting expression, $\langle Q \rangle_A / \langle Q \rangle_B = (N_p + 2 + 2/N_p)/3$, depends only on N_p, the label of the totally symmetric representation of $u_p(4)$ that sets the available Hilbert space for the rotovibrational degrees of freedom, thus giving an alternative to the usual methods of assessing this parameter [26].

III. EXPERIMENTAL DATA AND FIT RESULTS

We have extracted from the literature a total of 71 line positions, compiling a database that includes 55 IR transitions [12] and 16 INS transitions [15]. In these references, lines have been assigned with initial and final quantum numbers on the basis of experimental evidence and theoretical models.

The first step in the fitting procedure has been the assessment of the parameter N_p. As experimental data for the endohedrally confined species only involve $v = 0,1$ H_2 vibrational states, there is not enough information to estimate the N_p parameter for the hydrogen molecule. This parameter is usually fixed considering the ratio between first- and second-order parameters in the Dunham expansion for the molecule under study [26]. Therefore, we devised an alternative way to assess this parameter, using the rotovibrational spectroscopy of the free H_2 molecule making use of free H_2 vibrational data and explored the N_p dependence of the fit to the experimental energy terms beneath $10\,000$ cm^{-1} with a so(4) dynamical symmetry Hamiltonian

$$\hat{H}_{\text{so}(4)} = \beta\,\hat{C}_2[\text{so}(4)] + \gamma\,\hat{C}_2[\text{so}(3)] \qquad (14)$$
$$+ \gamma_2\hat{C}_2[\text{so}(3)]^2 + \kappa\,\hat{C}_2[\text{so}(3)]\hat{C}_2[\text{so}(4)].$$

The reason for setting an energy threshold is that the inclusion of highly excited energy levels, close to the molecular dissociation limit, implies the necessity of including continuum effects and resonances that are out of the scope of the vibron model, based on a u(4) compact Lie algebra [25,34,35]. The resulting root-mean-square (rms) deviation for a fit to a total of 31 rotovibrational experimental term energies from Refs. [36–38] is depicted as a function of N_p in Fig. 1, where it is clear that the best fit is obtained for $N_p = 34$ and the resulting parameters can be found in Table I.

With the value of N_p set to 34, we can return to the caged system. A PYTHON code has been developed to calculate the eigenvalues and eigenstates of the total Hamiltonian $\hat{H}_{\text{endo}}$ that encompasses the molecular rotovibrational degrees of freedom [Eq. (4)], the incarcerated center-of mass degrees of freedom [Eq. (9)], and the coupling between them in Eq. (12), and to compute the free parameter values that minimize the difference between calculated results and experimental line positions from Refs. [12,15]. The code makes use of SYMPY [39] and LMFIT [40] packages and is available upon request.
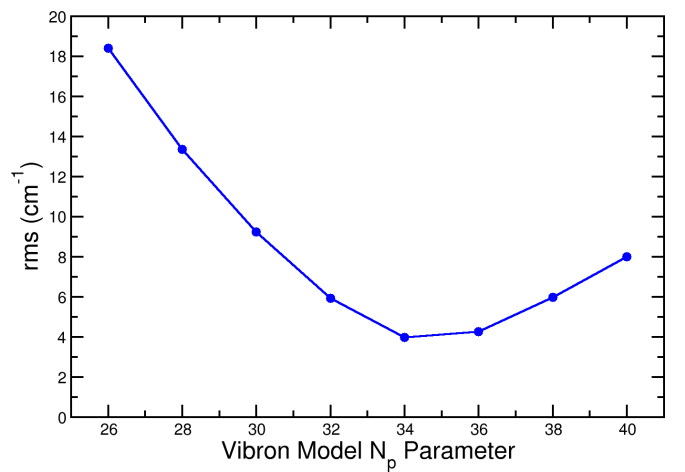

FIG. 1. Root-mean-square deviation for fits to free H_2 rotovibrational experimental term energies under a threshold value of $10\,000$ cm^{-1} with Hamiltonian (14) as a function of the number of vibrons parameter N_p.

TABLE I. Parameters of Hamiltonian (14) optimized to reproduce experimental term energies of the free H_2 molecule under $10\,000$ cm^{-1} with $N_p = 34$ and rms of the fit. Parameters are given in cm^{-1} units. The fit to 31 experimental energy levels has an rms $= 4.0$ cm^{-1}.

β	γ	γ_2	κ
1041.54(6)	32.80(7)	$-0.036215(7)$	0.72423(20)

In a preliminary set of calculations we have made several fits to the full data set and to different subsets, obtaining a good overall description. We have found that, leaving aside a constant energy shift, a minimal Hamiltonian that complies with all symmetry requirements and provides results that agree with experimental data has seven parameters: $\{\beta, \gamma, \kappa, a, b, c, \vartheta_{pq}\}$. The first three from Eqs. (5) and (6), the second three from Eq. (9), plus the low-order quadrupole coupling in Eq. (12). The fits with this set are denoted as F_0.

A finer fit, denoted as F_1, can be obtained with three more parameters, up to a total of ten free parameters. The three added parameters are γ_2 from Eq. (6), and the coupling parameters ϑ_{pqw} and v_{pq} of Eq. (12) associated with operators $\{\hat{C}_2[\mathrm{so}_p(4)][\hat{Q}_p^{(2)} \times \hat{Q}_q^{(2)}]^{(0)} + [\hat{Q}_p^{(2)} \times \hat{Q}_q^{(2)}]^{(0)}\hat{C}_2[\mathrm{so}_p(4)]\}$ and $\hat{C}_1[\mathrm{u}_q(3)]\hat{C}_2[\mathrm{so}_p(4)]$, respectively.

Preliminary calculations gave a satisfactory agreement with the experimental line positions, though some levels had a residual value much larger than expected from the overall fit agreement. This suggested that we consider a tentative reassignment of a set of five transitions showing unusually large deviations, as indicated in Table II. With this reassignment the quality of the fit has largely improved. The convenience of this reassignment in the framework of this model can be seen in Fig. 2 where the residuals for fits F_0 and F_1 are plotted as a function of the line position energy. The outcome for the original level assignment is shown in the upper panels, while the residuals with the new level assignment are depicted in the lower panels. The achieved improvement in the fit is remarkable though a deeper analysis is on the way to confirm these assignments and the findings will be published in a forthcoming paper [30]. In the following we refer to the set of experimental states with the five mentioned reassignments.

The final F_0 and F_1 parameters, with rms $= 3.1$ and 1.7 cm^{-1}, respectively, are given in Table III. The full list of residuals (experimental value minus calculated value) for
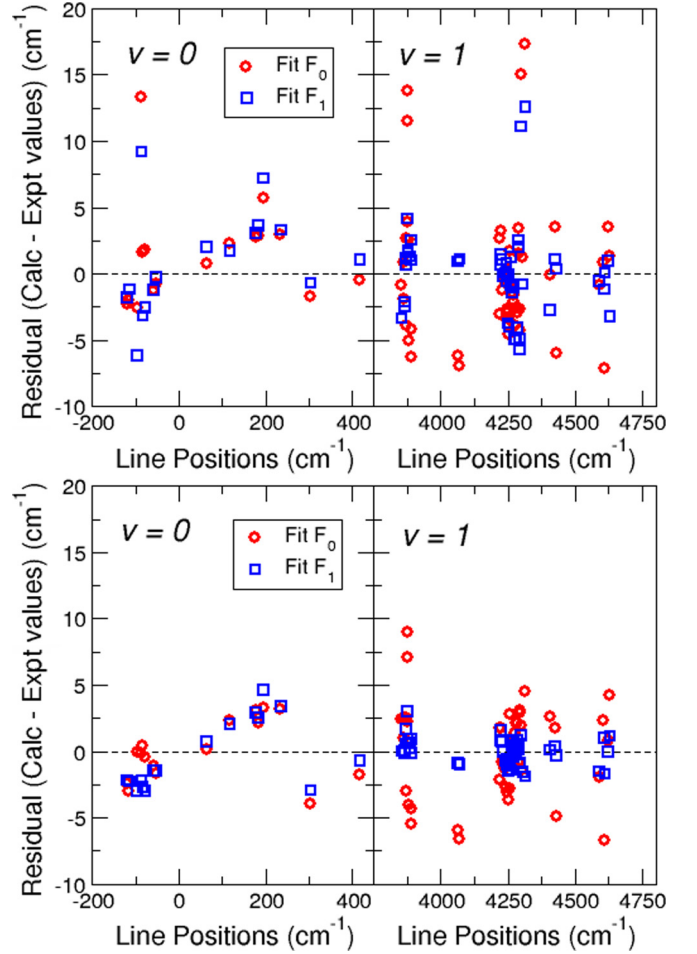

FIG. 2. Residuals of the F_0 and F_1 fits (see text) with the original assignments (upper panels) and including the changes suggested in Table II (lower panels).

both fits, plotted in Fig. 2, are given in Table IV together with the experimental line positions and initial and final state assignments.

The quality and robustness of our calculations allow us to estimate the energies of levels not yet accessed experimentally. We have included in Fig. 3 the calculated $v = 0, 1$, and 2 levels, the latter not yet measured. One can notice that with growing

TABLE II. Reassigned experimental transitions. Experimental states are given with the quantum numbers $vJN_qL\Lambda$. Line positions are given in cm^{-1} units.

Old assignment		New assignment			
Initial	Final	Initial	Final	Expt.	Ref.
00200	01111	00200	01110	-85.5	[15]
01221	11311	01334	11443	4294.8	[12]
00200	10311	01334	11445	4294.8	[12]
01334	11444	01221	11311	4300.0	[12]
01334	11445	01332	12312	4316.4	[12]

TABLE III. F_0 (minimal) and F_1 (finer) fit parameter values. In both cases $N_p = 34$. Hamiltonian parameters and rms are expressed in cm^{-1} units.

$\hat{H}_{\mathrm{u}_p(4)}$	β	γ	κ	γ_2
F_0	$-1083.23(18)$	58.09(17)	0.88(4)	
F_1	$-1081.72(15)$	58.28(20)	0.810(25)	$-0.032(15)$
$\hat{H}_{\mathrm{u}_q(3)}$	a	b	c	
F_0	178.3(8)	9.6(3)	$-3.26(15)$	
F_1	179.0(4)	8.46(17)	$-3.18(8)$	
$\hat{H}_{\mathrm{Coupl}}$	ϑ_{pq}	ϑ_{pqw}	v_{pq}	
F_0	0.94(7)			
F_1	0.86(5)	$-0.014(7)$	$-1.02(8)$	
rms	F_0	3.1	F_1	1.7

TABLE IV. Residuals for fits F_0 and F_1. Initial and final states are denoted by the quantum numbers of basis (1), $v J N_q L \Lambda$. Experimental states are extracted from Refs. [12,15] and reassigned transitions (see Table I) are highlighted in **red**. Both experimental line positions and residual values are expressed in cm^{-1}.

Initial	Final	Expt.	Calc. F_0	Calc. F_1	Initial	Final	Expt.	Calc. F_0	Calc. F_1
0 1 0 0 1	0 0 0 0 0	−118.6	−2.42	−2.16	0 1 0 0 1	1 1 1 1 1	4244.4	−2.76	−0.96
0 1 1 1 1	0 0 1 1 1	−113.7	−3.00	−2.27	0 2 1 1 2	1 2 2 2 3	4250.7	−0.65	−1.12
0 0 2 0 0	0 1 1 1 2	−95.7	−0.06	−3.00	0 1 0 0 1	1 1 1 1 2	4250.7	−3.14	−1.48
0 0 2 0 0	**0 1 1 1 0**	**−85.5**	**−0.17**	**−2.19**	0 0 0 0 0	1 0 1 1 1	4255.6	−3.649	−1.45
0 0 2 2 2	0 1 1 1 1	−82.7	0.44	−2.67	0 1 1 1 2	1 1 2 2 2	4255.6	−0.84	−0.82
0 0 2 2 2	0 1 1 1 2	−76.9	−0.44	−2.97	0 1 0 0 1	1 1 1 1 0	4261.3	−2.85	−1.43
0 2 0 0 2	0 1 1 1 1	−57.7	−1.09	−1.46	0 2 1 1 1	1 2 2 2 0	4261.3	2.77	0.83
0 2 0 0 2	0 1 1 1 2	−51.6	−1.66	−1.47	0 1 1 1 2	1 1 2 2 3	4267.1	0.64	0.43
0 1 0 0 1	0 0 1 1 1	65.2	0.15	0.73	0 1 1 1 1	1 1 2 2 1	4272.1	−1.05	−0.46
0 0 0 0 0	0 1 0 0 1	118.5	2.32	2.06	0 0 1 1 1	1 0 2 2 2	4272.1	0.25	0.72
0 1 0 0 1	0 1 1 1 1	178.8	3.05	2.91	0 1 2 2 2	1 1 3 3 3	4277.1	1.37	0.46
0 1 0 0 1	0 1 1 1 2	184.5	2.07	2.51	0 1 2 2 3	1 1 3 3 4	4281.2	2.12	0.05
0 1 0 0 1	0 1 1 1 0	196.0	3.26	4.61	0 0 2 2 2	1 0 3 3 3	4286.5	2.06	0.81
0 1 0 0 1	0 2 0 0 2	235.5	3.13	3.38	0 1 1 1 2	1 1 2 0 1	4290.2	0.62	0.55
0 0 0 0 0	0 1 1 1 0	304.9	−4.02	−2.92	0 0 1 1 1	1 0 2 0 0	4290.2	−0.79	0.14
0 1 0 0 1	0 2 1 1 1	417.8	−1.84	−0.71	**0 1 3 3 4**	**1 1 4 4 3**	**4294.8**	**2.82**	**−0.93**
0 1 2 0 1	1 1 1 1 2	3855.6	2.37	0.01	**0 1 3 3 4**	**1 1 4 4 5**	**4294.8**	**3.10**	**−0.83**
0 0 2 0 0	1 0 1 1 1	3866.0	1.0	0.08	**0 1 2 2 1**	**1 1 3 1 1**	**4300.0**	**1.91**	**1.19**
0 1 2 0 1	1 1 1 1 0	3866.0	2.45	−0.14	0 1 2 2 2	1 1 3 1 1	4306.7	−1.424	−1.570
0 2 1 1 3	1 2 0 0 2	3872.2	−3.04	0.59	**0 1 3 3 2**	**1 2 3 1 2**	**4316.4**	**4.45**	**−1.90**
0 1 2 2 1	1 1 1 1 1	3872.2	2.53	1.68	0 1 2 0 1	1 3 1 1 2	4407.4	2.63	0.11
0 1 3 3 3	1 1 2 2 2	3876.0	8.92	3.02	0 1 2 2 3	1 3 1 1 4	4426.8	1.77	0.39
0 0 3 3 3	1 0 2 2 2	3878.6	7.04	0.67	0 1 1 1 2	1 3 0 0 3	4431.9	−4.94	−0.30
0 1 2 2 3	1 1 1 1 2	3878.6	2.25	0.96	0 0 0 0 0	1 2 1 1 1	4592.0	−2.02	−1.53
0 0 2 2 2	1 0 1 1 1	3884.9	0.72	0.20	0 0 1 1 1	1 2 2 2 1	4608.9	2.25	1.02
0 1 1 1 2	1 1 0 0 1	3884.9	−4.08	0.62	0 1 0 0 1	1 3 0 0 3	4612.5	−6.77	−1.69
0 1 1 1 1	1 1 0 0 1	3891.3	−4.36	0.92	0 0 1 1 1	1 2 2 0 2	4624.3	0.76	−0.06
0 0 1 1 1	1 0 0 0 0	3891.3	−5.49	−0.16	0 0 2 2 2	1 2 3 3 1	4630.0	4.24	1.14
0 1 0 0 1	1 1 0 0 1	4065.4	−6.01	−0.86	0 1 0 0 1	1 3 1 1 2	4802.6	−2.77	−1.28
0 0 0 0 0	1 0 0 0 0	4071.4	−6.62	−0.96	0 1 1 1 2	1 3 2 2 2	4814.8	0.13	−0.17
0 3 0 0 3	1 3 1 1 4	4223.3	1.70	0.76	0 1 1 1 1	1 3 2 2 2	4821.6	0.26	0.53
0 0 1 1 1	1 2 0 0 2	4223.3	−2.20	1.57	0 1 1 1 1	1 3 2 2 1	4829.7	1.29	1.40
0 3 0 0 3	1 3 1 1 2	4226.2	1.74	0.73	0 1 1 1 2	1 3 2 0 3	4836.2	1.68	1.74
0 2 0 0 2	1 2 1 1 2	4233.1	−0.82	−0.04	0 1 2 2 2	1 3 3 3 1	4846.4	1.83	0.35
0 2 0 0 2	1 2 1 1 3	4239.8	−1.34	−0.72	0 1 2 2 1	1 3 3 1 2	4864.5	−0.96	−2.24
0 2 0 0 2	1 2 1 1 1	4244.4	−1.07	−0.56					

v, the higher the J the bigger the negative energy shift of corresponding states. An extensive table with all calculated levels for $v = 0, 1, 2$ vibrational quanta with $N_q \leqslant 4$ and $\Lambda \leqslant 5$ can be found in the Supplemental Material [41]. In addition to the term energy, expressed in cm^{-1} units, we also indicate in the table the probability of the largest component (squared coefficient) of the corresponding eigenstate expressed in basis (1).

IV. SUMMARY AND CONCLUSIONS

In summary, we have introduced a u(4) ⊕ u(3) algebraic scheme that combines the vibron model description of a diatomic molecule rotovibrational structure with an algebraic description of the motion of the molecule center of mass inside an isotropic cage. This model is mathematically rich and has a large number of possible terms that can be attributed to different physical mechanisms. We have presented here a discussion of a few selected physical mechanisms that, in spite of the model's simplicity, give insight into the spectroscopic properties of diatomic endohedrally confined molecules. We have then applied the symmetry-guided scheme to a database of experimental lines, finding a very good overall agreement to the experimental line positions and finding that the fits improve considerably upon reassigning the quantum numbers of a small subset of energy levels.

The next step is the inclusion of transition intensities in the model and the enrichment of the approach, which could take place in one of two possible venues, either by defining an embedding $u_{pq}(7) \supset u_p(4) \oplus u_q(3)$ dynamical algebra or by a dynamical algebra $u_p(4) \oplus u_q(4)$ with results that will be published soon [30]. Another venue for future research is the inclusion in the algebraic model of the cage icosahedral symmetry effect on the spectrum, which has recently been investigated [18,20].
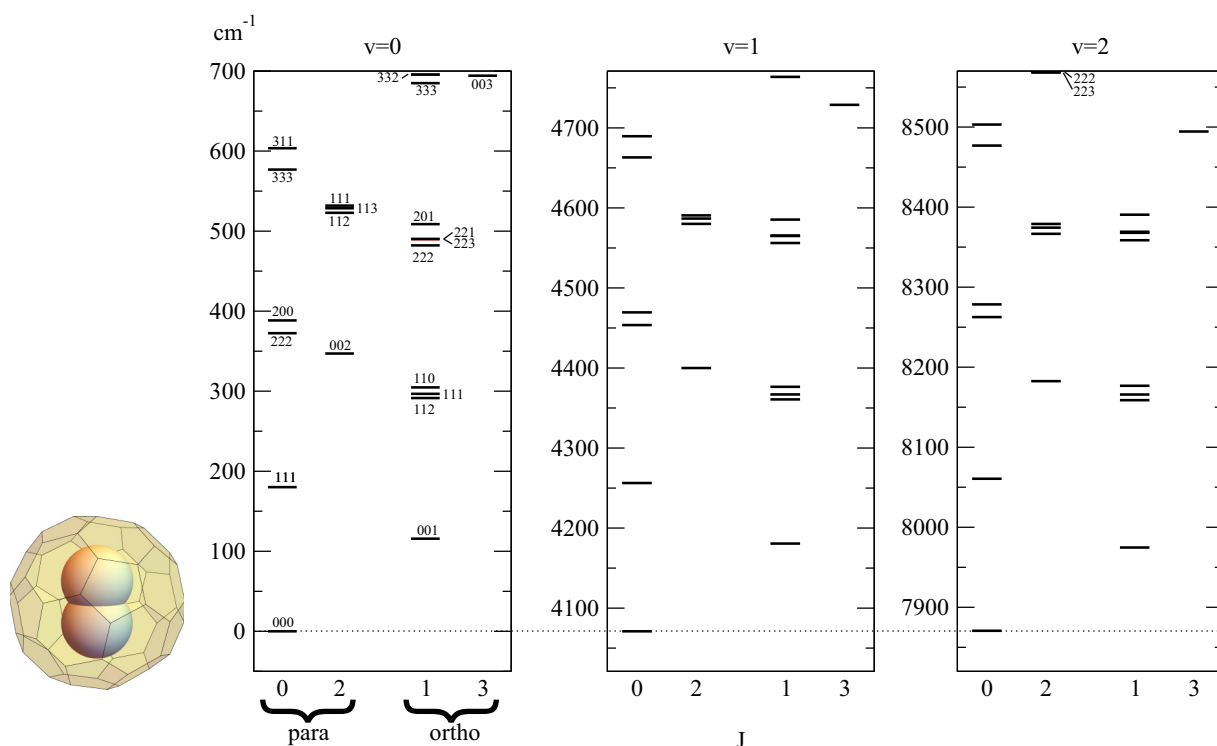
FIG. 3. Theoretical rotovibrational spectrum of $H_2@C_{60}$. The three cuts show the energy levels in a 700 cm^{-1} wide energy window just above the three lowest vibrational excitations $v = 0, 1$, and 2. States are further divided into *para* (left) and *ortho* (right) states and are labeled by J on the horizontal axis and $N_q L \Lambda$ on each state. These quantum numbers are repeated with the same order in each panel, except where noted.

[1] Y. Chai, T. Guo, C. Jin, R. E. Haufler, L. P. F. Chibante, J. Fure, L. Wang, J. M. Alford, and R. E. Smalley, J. Phys. Chem. **95**, 7564 (1991).

[2] S. Ito, H. Shimotani, H. Takagi, and N. Dragoe, Fullerenes, Nanotubes, Carbon Nanostruct. **16**, 206 (2008).

[3] M. H. Levitt and A. J. Horsewill, Phil. Trans. Math. Phys. Eng. Sci. **371**, 20130124 (2013).

[4] K. Komatsu, Phil. Trans. Math. Phys. Eng. Sci. **371** (2013).

[5] K. Komatsu, M. Murata, and Y. Murata, Science **307**, 238 (2005).

[6] K. Kurotobi and Y. Murata, Science **333**, 613 (2011).

[7] A. Krachmalnicoff *et al.*, Nat. Chem. (2016).

[8] N. J. Turro, J. Y.-C. Chen, E. Sartori, M. Ruzzi, A. Marti, R. Lawler, S. Jockusch, J. López-Gejo, K. Komatsu, and Y. Murata, Acc. Chem. Res. **43**, 335 (2010).

[9] S. Mamone, J. Y.-C. Chen, R. Bhattacharyya, M. H. Levitt, R. G. Lawler, A. J. Horsewill, T. Rõõm, Z. Bačić, and N. J. Turro, Coord. Chem. Rev. **255**, 938 (2011).

[10] M. Carravetta, A. Danquigny, S. Mamone, F. Cuda, O. G. Johannessen, I. Heinmaa, K. Panesar, R. Stern, M. C. Grossel, A. J. Horsewill, A. Samoson, M. Murata, Y. Murata, K. Komatsu, and M. H. Levitt, Phys. Chem. Chem. Phys. **9**, 4879 (2007).

[11] S. Mamone, M. Ge, D. Hüvonen, U. Nagel, A. Danquigny, F. Cuda, M. C. Grossel, Y. Murata, K. Komatsu, M. H. Levitt, T. Rõõm, and M. Carravetta, J. Chem. Phys. **130**, 081103 (2009).

[12] M. Ge, U. Nagel, D. Hüvonen, T. Rõõm, S. Mamone, M. H. Levitt, M. Carravetta, Y. Murata, K. Komatsu, J. Y.-C. Chen, and N. J. Turro, J. Chem. Phys. **134**, 054507 (2011).

[13] T. Rõõm, L. Peedu, M. Ge, D. Hüvonen, U. Nagel, S. Ye, M. Xu, Z. Bačić, S. Mamone, M. H. Levitt, M. Carravetta, J.-C. Chen, X. Lei, N. J. Turro, Y. Murata, and K. Komatsu, Phil. Trans. Math. Phys. Eng. Sci. **371** (2013).

[14] A. J. Horsewill, S. Rols, M. R. Johnson, Y. Murata, M. Murata, K. Komatsu, M. Carravetta, S. Mamone, M. H. Levitt, J. Y.-C. Chen, J. A. Johnson, X. Lei, and N. J. Turro, Phys. Rev. B **82**, 081410 (2010).

[15] A. J. Horsewill, K. S. Panesar, S. Rols, J. Ollivier, M. R. Johnson, M. Carravetta, S. Mamone, M. H. Levitt, Y. Murata, K. Komatsu, J. Y.-C. Chen, J. A. Johnson, X. Lei, and N. J. Turro, Phys. Rev. B **85**, 205440 (2012).

[16] A. J. Horsewill, K. Goh, S. Rols, J. Ollivier, M. R. Johnson, M. H. Levitt, M. Carravetta, S. Mamone, Y. Murata, J. Y.-C.

Chen, J. A. Johnson, X. Lei, and N. J. Turro, Phil. Trans. Math. Phys. Eng. Sci. **371**, 20110627 (2013).

[17] M. Xu, M. Jiménez-Ruiz, M. R. Johnson, S. Rols, S. Ye, M. Carravetta, M. S. Denning, X. Lei, Z. Bačić, and A. J. Horsewill, Phys. Rev. Lett. **113**, 123001 (2014).

[18] S. Mamone, M. R. Johnson, J. Ollivier, S. Rols, M. H. Levitt, and A. J. Horsewill, Phys. Chem. Chem. Phys. **18**, 1998 (2016).

[19] M. Xu, S. Ye, and Z. Bačić, J. Phys. Chem. Lett. **6**, 3721 (2015).

[20] B. Poirier, J. Chem. Phys. **143**, 101104 (2015).

[21] M. Xu, F. Sebastianelli, Z. Bačić, R. Lawler, and N. J. Turro, J. Chem. Phys. **128**, 011101 (2008).

[22] M. Xu, F. Sebastianelli, Z. Bačić, R. Lawler, and N. J. Turro, J. Chem. Phys. **129**, 064313 (2008).

[23] M. Xu, L. Ulivi, M. Celli, D. Colognesi, and Z. Bačić, Phys. Rev. B **83**, 241403(R) (2011).

[24] M. Xu and Z. Bačić, Phys. Rev. B **84**, 195445 (2011).

[25] F. Iachello, Chem. Phys. Lett. **78**, 581 (1981).

[26] F. Iachello and R. D. Levine, *Algebraic Theory of Molecules*, Topics in Physical Chemistry Series (Oxford University, Oxford, 1994).

[27] A. Frank and P. Van Isacker, *Symmetry Methods in Molecules and Nuclei* (S y G Editores, Mexico City, 2005).

[28] F. Iachello, *Lie Algebras and Applications*, Lecture Notes in Physics, Vol. 891 (Springer, Berlin, 2015).

[29] R. Bijker, F. Iachello, and A. Leviatan, Ann. Phys. (NY) **236**, 69 (1994).

[30] F. Pérez-Bernal and L. Fortunato (unpublished).

[31] M. Xu, S. Ye, A. Power, R. Lawler, N. J. Turro, and Z. Bačić, J. Chem. Phys. **139**, 064309 (2013).

[32] A. Shalit and I. Talmi, *Nuclear Shell Theory* (Academic, New York, 1963).

[33] A. R. Edmonds, *Angular Momentum in Quantum Mechanics*, Reissue ed. (Princeton University, Princeton, NJ, 1996).

[34] F. Iachello and R. D. Levine, J. Chem. Phys. **77**, 3046 (1982).

[35] S. Kim, I. Cooper, and R. Levine, Chem. Phys. **106**, 1 (1986).

[36] I. Dabrowski, Can. J. Phys. **62**, 1639 (1984).

[37] M. Stanke, D. Kędziera, S. Bubin, M. Molski, and L. Adamowicz, J. Chem. Phys. **128**, 114313 (2008).

[38] E. J. Salumbides, G. D. Dickenson, T. I. Ivanov, and W. Ubachs, Phys. Rev. Lett. **107**, 043005 (2011).

[39] SymPy Development Team, SymPy: Pyphon library for symbolic mathematics, 2016.

[40] M. Newville, T. Stensitzki, D. B. Allen, and A. Ingargiola, LMFIT: Non-linear least-square minimization and curve-fitting for Python, 2014.

[41] See Supplemental Material at http://link.aps.org/supplemental/10.1103/PhysRevA.94.032508 for a table of calculated $H_2@C_{60}$ levels for $v = 0,1,2$; $N_q \leqslant 4$; and $\Lambda \leqslant 5$.